IEEE Transactions on Nuclear Science, Vol.NS-24, No.3, June 1977

TUNING THE BEAM SHAPING SECTION OF THE LAMPF BIOMEDICAL CHANNEL

M. A. Paciotti, J. N. Bradbury, R. L. Hutson, E. A. Knapp and O. M. Rivera
University of California
Los Alamos Scientific Laboratory
Los Alamos, New Mexico

D. Laubacher
Purdue University
Lafayette, Indiana

The Biomedical Channel at LAMPF is used for radiotherapy with negative pi mesons. We have previously reported the results of the tuning of the first section of the channel.[1] Here we discuss our understanding of the transport properties of the beam-shaping section of the channel. Large emittance beams produced by the first section are matched to specific output requirements by tuning the last five quadrupole magnets using a combination of measurements and calculations.

Quadrupole Magnet Description

The beam-shaping section of the channel consists of five short identical quadrupole magnets, Q4 through Q8, delivering a vertical beam to the treatment room. The bores are 35.56 cm, and the physical lengths are 27.94 cm. The effective lengths are 0.433 m, and the center to center separations are 0.84 m. Including a 0.9 m drift after Q8, the total length is 4.7 m. At 800 A the pole tip field is 7 kG. Saturation effects are apparent in the magnetization curve above 400 A.

Channel Tuning

Measurement Technique

Multiwire proportional counters located above Q4 and below Q8 determine the position and angle in both planes for each particle traversing the channel. BM3, the last bending magnet in the channel is located above Q4 and serves as a magnetic spectrometer. Using chambers before and after BM3, the momentum of the particle is measured, completing the information for the event.[1]

A sample of the information obtained is displayed in figures 1 through 3 for a beam (Run 428) developed and used for pion therapy. Figure 1 is the uncollimated X-profile of the beam at a drift of 0.9m from the effective edge of Q8. A gaussian fit is applied to the distribution yielding a σ, or rms, of 7.5 cm. The fitting procedure weights the fit by the gaussian itself. Figure 2 is the Y-profile; σ is 5.9 cm.

The two dimensional phase space X-θ is displayed in Fig. 3. The numbers in the display represent the number of events per bin as a power of 2. The one and two standard deviation ellipses are drawn. The correlation between X and θ is taken from the fitted ellipse. The beam information is summarized in the first column of Table I; note the very large emittances involved. Flat rather than gaussian-shaped beams are desired for treatment, and experience with the computer design of the first collimator showed that an adequately flat field could be obtained by collimating a diverging beam. Treatment tunes, such as Run 428, diverge in both planes. Collimation of a large beam to a smaller size necessarily reduces the useful number of pions. These losses have been accepted to gain field flatness.

Q4-Q8 Optimization

The process of finding a new beam consists of a number of steps. 1) Starting with an approximate input phase space at the top of Q4, a TRANSPORT[2] run finds the new quad fields. 2) These quad strengths are set up on the channel, and the output beam is measured. 3) Derivatives of beam sizes and waist positions are experimentally determined with respect to quad currents. We consider variations of each quad current and variations of all pairs of currents. 4) Usually a satisfactory beam is obtained within one or two iterations.

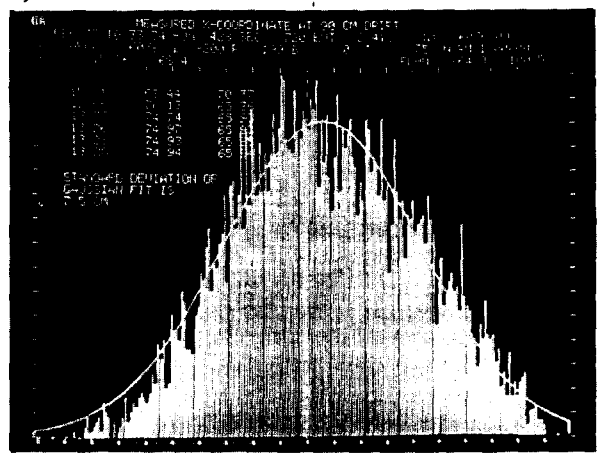

Figure 1: Uncollimated measured X-profile of beam at 0.9 m drift from Q8. Scale is ± 20 cm. σ = 7.5 cm.

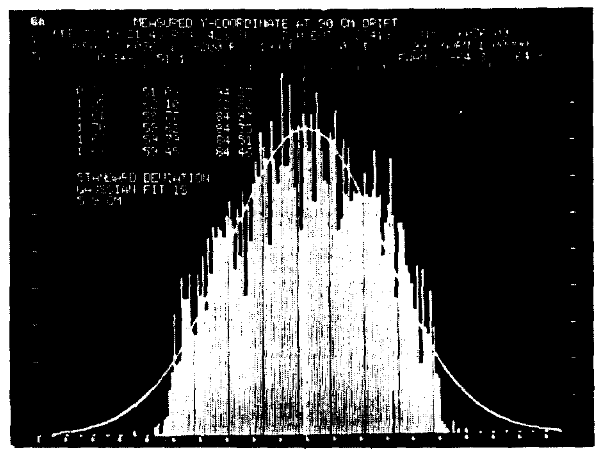

Figure 2: Uncollimated measured Y-profile of beam at 0.9 m drift from Q8. Scale is ± 20 cm. σ = 5.9 cm.

Transformation Matrices for Quads

It is important to understand the transformation properties of the last section so that the code TRANSPORT[2] can find solutions directly. Required is a set of effective lengths and of magnetization curves that accurately simulate Q4-Q8.

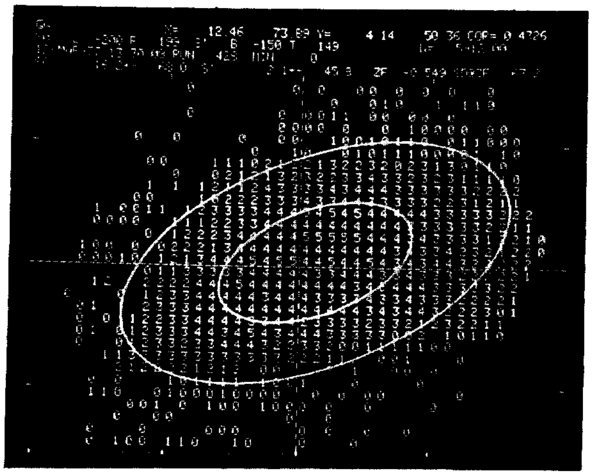

Figure 3: X-θ phase space diverging at 0.9 m drift from Q8. Correlation is 0.43. Scale is ± 20 cm by ± 150 mr.

Magnetic Field Measurements

Measurements have been made for each of the last quads isolated from any nearby iron. Measurements on Q8 installed below Q7 show that both $\int \mathrm{Grad}\cdot d\ell$ and effective length are modified by the adjacent iron. The effective length is reduced from 0.433 m to 0.418 m.

Direct Matrix Element Measurement

Measurement of particle trajectories above and below the beam-shaping section allows a determination of the first-order matrix elements. The transformation is found between the U-V plane defined at the upper effective edge of Q4 and the X-Y plane defined at 0.9 m below the effective edge of Q8. For each particle, the quantity X/U, for example, is histogrammed. Where the angles U' are small, X/U is R11, the first-order matrix element. The distribution of X/U is approximately gaussian, the centroid of which we take as R11. Cuts on U' of various widths are made, and the extrapolation of R11 to zero width on U' is the best value of R11. For Run 428 we find the first-order transformation

$$R = \begin{pmatrix} -0.19 & -0.17 & & \\ 4.8 & -0.72 & & \\ & & 0.49 & 0.19 \\ & & -2.9 & 0.50 \end{pmatrix}.$$

The X-plane determinant is 0.95. However the Y-plane determinant is 0.80, indicating that significant errors exist in this approach.

Ray Tracing

The on-line analysis code does a second-order ray trace from the U-V plane to the X-Y plane. The TRANSPORT matrices come from the quad currents and the effective lengths which can be adjusted on line. For every particle trajectory at the U-V plane the trajectory at the X-Y plane is predicted. These calculated vectors X_c, θ_c, Y_c, and ϕ_c are histogrammed and compared with the measured vectors X, θ, Y, and ϕ. By way of comparison we define $\Delta_x = X-X_c$, $\Delta_\theta = \theta-\theta_c$, $\Delta_Y = Y-Y_c$, and $\Delta_\phi = \phi-\phi_c$. If the Δ's are small then the quad fields and effective lengths have been determined sufficiently well. Using the field measurement data directly, the widths of the Δ distributions are not impressively narrow. The agreement between TRANSPORT predictions and measured beams is not yet good enough so that TRANSPORT can be used to best advantage in the design of new beams.

Changing the central momentum input to the matrix calculation produces marked narrowing of the widths of the Δ distributions ; we examine the behavior of the widths as a function of

$$\text{the factor } f = \frac{\text{measured central momentum of beam}}{\text{central momentum in matrix calculation}}.$$

Figure 4 shows the dependence of the widths of the differences on the factor f for Run 378. Dozens of such plots have been made for the widest variety of tunes available. If each of the four curves for all of these tunes minimizes at roughly the same factor f, then we have a consistent set of fields, lengths, and central momenta. The minima are occuring at a value of f less than 1.0, about 0.96. A higher value is needed for the central momentum input to the matrix calculation than is measured by the BM3 spectrometer.

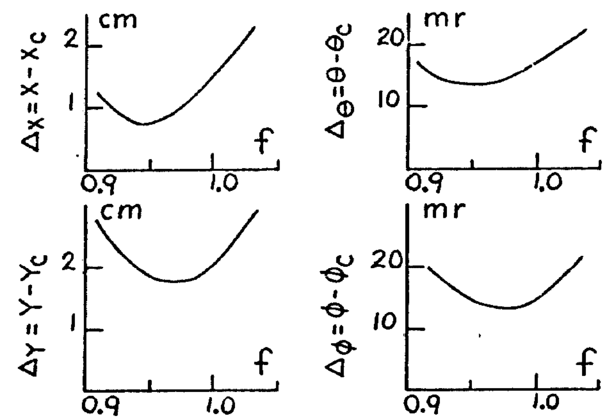

Figure 4: σ's of differences between measured and calculated beam coordinates vs. central momentum scaling factor (Run 389).

For Figure 4 the pole tip fields for Q4 and Q8 were increased by 2% and 3% respectively in the matrix calculation above the values as determined from the field measurements. The effective lengths of these magnets are already longer than the others due to the fact that the outer effective edges of these magnets are not adjacent to another magnet. This increase in Q4 and Q8 fields has a beneficial effect in making the minima for the two planes occur at closer to the same scale factor f of about 0.96. This property is true for three different polarity configurations and for a wide variety of tunes.[3]

RMS Beam Envelope Comparisons

Figure 4 says that for Run 389 the TRANSPORT matrices (at 0.96 momentum factor) predict X to 0.8 cm rms; θ to 13 mr rms; Y to 1.7 cm rms; and ϕ to 14 mr rms. Table II summarizes the rms beam envelope information for Run 389, one of our smallest beams. The first column contains the measured beam parameters. Comparing, the ray trace predicts X to 0.8 cm within a 2.7 cm beam, a good performance. Y is found to 1.7 cm within a 3.4 cm beam, not as good.

However, the rms envelope of the matrix calculated rays is in very good agreement with the measured beam. (Compare columns 1 and 2.) Listed are beam sizes, angular sizes, correlation parameters between position and angle, and correlation parameters between position and momentum as well as angle and momentum. The Z positions of the waists are listed relative to the X-Y plane.

The rms envelope of the beam at the U-V plane with all correlations is input to a second-order TRANSPORT calculation using the same matrix as for the ray traced beam. The σ-matrix output of the TRANSPORT calculation is listed in the third column. Table I contains the same results from Run 428, one of the largest beams. The good agreement between measurement and TRANSPORT calculation means that new beams can be designed using TRANSPORT provided that the phase space at the U-V plane can be determined sufficiently well. A scheme of iteration with a starting phase space at the U-V plane from a similar tune should work. The input beam changes due to a different portion of a larger phase space being accepted into Q4-Q8. These changes are not large when the Q4-Q8 polarities are not changed.

The Run 428 first-order matrix used for the above calculation is

$$R = \begin{pmatrix} -0.179 & -0.166 & & \\ 5.230 & -0.745 & & \\ & & 0.475 & 0.217 \\ & & -3.424 & 0.542 \end{pmatrix} .$$

This R matrix is reasonably close to the measured one given earlier. Second-order matrix elements are not important as the momentum spread for this beam is only 1.9% $\Delta p/p$ (rms).

References

[1] M.A. Paciotti, J.N. Bradbury, J.A. Helland, R.L. Hutson, E.A. Knapp, and O.M. Rivera, "Tuning of the First Section of the Biomedical Channel at LAMPF", IEEE Trans. on Nucl. Sci. Vol. NS-22, No. 3 (1975).

[2] K.L. Brown and S.K. Howry, "TRANSPORT/360, A Computer Program for Designing Charged Particle Beam Transport Systems," SLAC-91 (1970).

[3] We have chosen to alter the central momentum input to the matrix calculation rather than making the equivalent change to the pole tip fields. Independent measurements on the beam indicate that the BM3 spectrometer underestimates the central momentum of the beam by up to a few percent. Such a calibration systematic in BM3 offers a possible explanation for the 4% shift we observe in the minima of the σ's of the Δ distributions. We await a beam momentum measurement to resolve this question. It is also true that when the effective lengths are scaled instead of the central momentum, the minima of the σ's of the Δ distributions occur at the same scaling factor, about 0.96. Likewise we can substitute a 2% and 3% increase in the effective lengths of Q4 and Q8 for the corresponding pole tip field increases we have used in the text. Our method is not sensitive enough to distinguish between a change in pole tip field and the same change in effective length.

Table I Run 428 - Envelope Comparisons at 0.90 m Drift Distance

	rms envelope of measured beam	rms envelope of matrix calculated rays	rms envelope from TRANSPORT
X	7.5 cm	6.3 cm	6.1 cm
θ	49 mr	49 mr	52 mr
r(21)	0.43	0.37	0.33
X waist position	-66 cm	-48 cm	-39 cm
X emittance	332π cm mr	287π cm mr	299π cm mr
Y	5.9 cm	5.6 cm	5.6 cm
φ	23 mr	20 mr	21 mr
r(43)	0.49	0.51	0.52
Y waist position	-126 cm	-143 cm	-139 cm
Y emittance	118π cm mr	96π cm mr	100π cm mr
r(61)	-0.46	-0.46	-0.38
r(62)	-0.26	-0.25	-0.23

Table II Run 389 - Envelope Comparisons at 0.90 m Drift Distance

	rms envelope of measured beam	rms envelope of matrix calculated rays	rms envelope from TRANSPORT
X	2.7 cm	2.4 cm	2.4 cm
θ	116 mr	122 mr	130 mr
r(21)	0.18	0.30	0.31
X waist position	-4.2 cm	-5.9 cm	-5.7 cm
X emittance	308π cm mr	279π cm mr	297π cm mr
Y	3.4 cm	3.8 cm	3.9 cm
φ	30 mr	22 mr	24 mr
r(43)	0.18	0.01	0.08
Y waist position	-20.4 cm	-1.7 cm	-13.0 cm
Y emittance	100π cm mr	84π cm mr	93π cm mr
r(61)	-0.41	-0.49	-0.40
r(62)	-0.21	-0.24	-0.28